

## Selective enantioseparation of levocetirizine via a hollow fiber supported liquid membrane and mass transfer prediction

Niti Sunsandee\*, Natchanun Leepipatpiboon\*\*, and Prakorn Ramakul\*\*\*†

\*Government Pharmaceutical Organization, Ratchathevi, Bangkok 10400, Thailand

\*\*Chromatography and Separation Research Unit, Department of Chemistry, Faculty of Science, Chulalongkorn University, Patumwan, Bangkok 10330, Thailand

\*\*\*Department of Chemical Engineering, Faculty of Engineering and Industrial Technology, Silpakorn University, Nakhon Pathom 73000, Thailand

(Received 2 January 2013 • accepted 28 March 2013)

**Abstract**—The enantioselective separation of levocetirizine via a hollow fiber supported liquid membrane was examined. *O,O'*-dibenzoyl-(2*R*,3*R*)-tartaric acid ((-)-DBTA) diluted in 1-decanol was used as a chiral selector extractant. The influence of concentrations of feed and stripping phases, and extractant concentration in the membrane phase, was also investigated. A mathematical model focusing on the extraction side of the liquid membrane system was presented to predict the concentration of levocetirizine at different times. The extraction and recovery of levocetirizine from feed phase were 75.00% and 72.00%, respectively. The mass transfer coefficients at aqueous feed boundary layer ( $k_f$ ) and the organic liquid membrane phase ( $k_m$ ) were calculated as  $2.41 \times 10^2$  and  $1.89 \times 10^2$  cm/s, respectively. The validity of the developed model was evaluated through a comparison with experimental data, and good agreement was obtained.

Key words: Levocetirizine, (-)-DBTA, Liquid Membrane, Hollow Fiber, Enantioselective Separation

### INTRODUCTION

The prevalence of allergic disease is increasing worldwide. The World Health Organization (WHO) estimates that 10-25% of the population worldwide is affected by allergic rhinitis (AR) and allergic skin disease [1]; chronic urticaria is reported to affect 25% of people at some point in their lives [2]. Chronic idiopathic urticaria (CIU) is estimated to affect between 0.1-3.0% of the population in Europe and the USA. It is thought that the worldwide lifelong prevalence of CIU is 0.5% across different populations [3].

Cetirizine ((±)-[2-[4-[(4-chlorophenyl)methyl]-1-piperazinyl]ethoxy]acetic acid) is a potent, long-acting, second-generation histamine  $H_1$  receptor antagonist used for the treatment of urticaria and allergic rhinitis [4-6]. Thus, cetirizine has the advantage of lacking the CNS depressant effects frequently encountered in other antihistamines [7]. Cetirizine is the acid metabolite of hydroxyzine and has the structure of this zwitterionic drug. Three ionizable functions are present in the structure: a strong acid group ( $pK_a=2.9$ ), a strong basic group ( $pK_a=8.0$ ) and a weak basic group ( $pK_a=2.2$ ) [8-10]. Cetirizine is a racemic mixture of *S*- and *R*-enantiomers. The *R*-enantiomer, levocetirizine, in Fig. 1(a), carries the majority of the histamine  $H_1$ -receptor blocking activity [11].

Levocetirizine, a eutomer, is the most potent antihistamine with an approximately 30-fold higher affinity for the human  $H_1$ -receptor than dextrocetirizine, as shown in Fig. 1(b) [12]. Levocetirizine blocks histamine receptors [12]; it does not prevent the actual release of histamine from mast cells but prevents binding to its receptors [13]. This in turn prevents the release of other allergy chemicals and in-

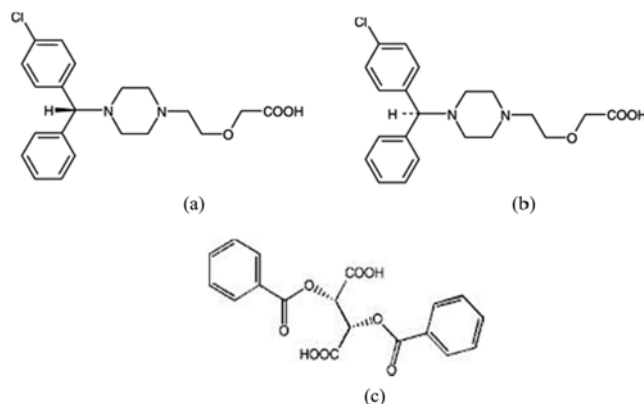


Fig. 1. The structures of (a) levocetirizine, (b) dextrocetirizine, (c) *O,O'*-dibenzoyl-(2*R*,3*R*)-tartaric acid ((-)-DBTA).

creased blood supply to the area, and provides relief from the typical symptoms of hay fever [14]. It is more effective with fewer side effects than the second-generation histamine [15]. Furthermore, the pharmacokinetic behavior of levocetirizine appears more favorable due to a lower volume of distribution and a slower renal clearance [16].

Enantiomeric separation of cetirizine is a very important method for preparative separation of enantiomers. In particular, many researchers have attempted to separate levocetirizine from its racemic mixture via crystallization [17], enzymatic conversion [18], chromatography [19] and capillary electrophoresis [20]. Unfortunately, these separation processes have some serious disadvantages. The most often employed isolation of levocetirizine involves selective diastereomeric salt crystallization, but this technique requires many

†To whom correspondence should be addressed.  
E-mail: prakorn@su.ac.th

time-consuming and expensive steps, increasing the complexity of the process and leading to a considerable loss of product [21]. Enzymatic conversion is expensive due to its single action [22], and chromatography is not suitable due to its production scale. To avoid the problems above, asymmetric synthesis and kinetic resolution have been developed. However, the cost of this process is high and a long operating time is required to develop a proper route for all chiral compounds.

Liquid membranes have shown great potential, especially in cases where solute concentrations are relatively low and other techniques cannot be applied efficiently, since they combine the process of extraction and stripping in a single unit operation. The use of a hollow fiber supported liquid membrane (HFSLM) is the most popular method, which can be easily performed automatically and continuously with good effect, high recovery and low energy consumption. HFSLM technique has specific characteristics of simultaneous extraction and stripping processes of low concentrations of the target species in one single stage [23]. Some other advantages of HFSLM over traditional separation techniques include lower capital and operating costs [24], lower energy consumption [25], low amount of solvent used, and high selectivity [26]. Actually, liquid membranes have been used in the separation of metal ions, organic compounds and in enzymatic transformation [27-29]. Therefore, the separation of enantiomers by HFSLM is of great interest. In addition, in recent years racemic separations by liquid membranes and chiral solid membranes have been performed, and good results were obtained [28-30].

In this work, the selective separation of levocetirizine by using HFSLM with *O,O'*-dibenzoyl-(2*R*,3*R*)-tartaric acid ((-)-DBTA) as

a chiral extractant was examined, as shown in Fig. 1(c). The separation factor ( $\alpha$ ) and the percentage enantiomeric excess (% *e.e.*) are first recorded. Not only was the separation of levocetirizine investigated by HFSLM, but the mathematical model was also studied to determine the mass transfer coefficients ( $k_f$  and  $k_m$ ). Eventually, mass transfer theory was used to establish the equation to predict the concentration of levocetirizine in the feed tank as a function of time, and it was compared with experimental results.

## THEORY

The HFSLM system consists of a feed phase, organic membrane phase and stripping phase. The feed phase and stripping phase are in contact with the organic membrane phase. The organic membrane phase consists of carriers embedded in porous material to enhance separation. Transportation of levocetirizine occurs as a consequence of the concentration driving force between the two opposite sides of aqueous phase.

The organic phase is filled in the pores of fibers by capillary force, acting as a barrier between the feed and stripping solutions. The chiral selector *O,O'*-dibenzoyl-(2*R*,3*R*)-tartaric acid ((-)-DBTA) is trapped in the hydrophobic microporous hollow fiber module. The levocetirizine forms enantioselective complexes with (-)-DBTA by hydrogen bonding in the liquid membrane. Previous partitioning experiments [30] indicate that the levocetirizine-(-)-DBTA complex dissolves in the membrane phase, whereas dextrocetirizine prefers to remain in the feed phase. The transport mechanism of levocetirizine through the liquid membrane is shown in Fig. 2.

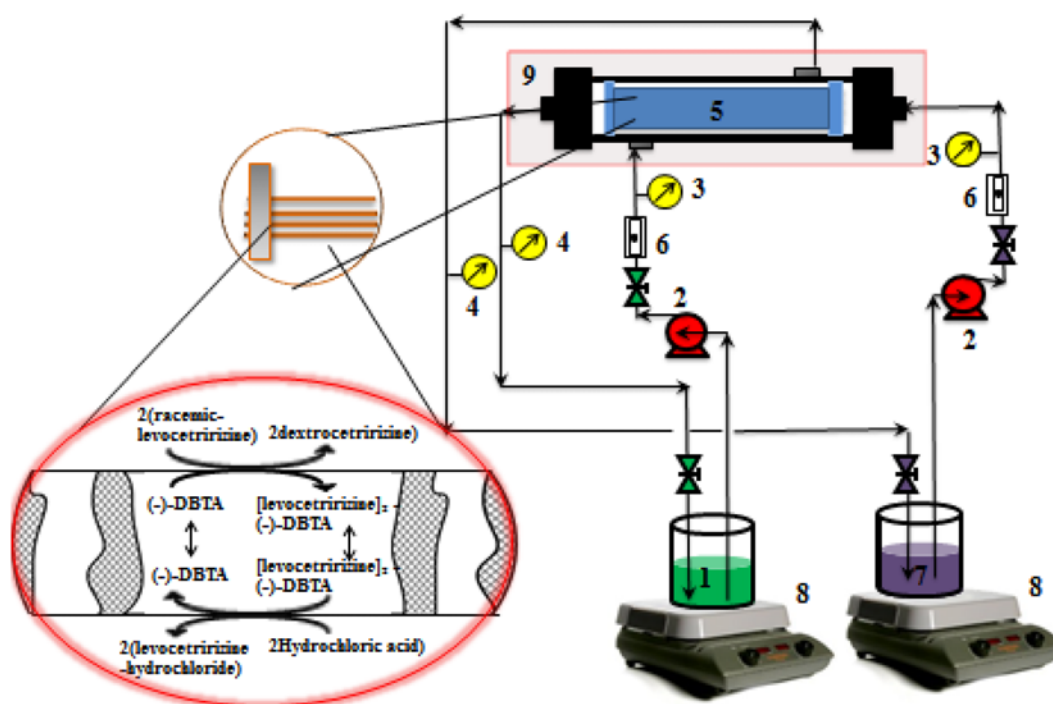


**Fig. 2. Schematic representation of the counter-current flow diagram for batch mode operation in HFSLM and counter transport mechanism of levocetirizine using (-)-DBTA as the chiral selective extractant.**

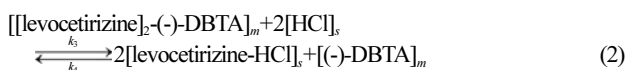
- |                          |                           |                                     |                            |
|--------------------------|---------------------------|-------------------------------------|----------------------------|
| 1. Feed reservoir        | 4. Outlet pressure gauges | 7. Stripping reservoir              | 9. Temperature control box |
| 2. Gear pumps            | 5. Hollow fiber module    | 8. Stirrer with temperature control |                            |
| 3. Inlet pressure gauges | 6. Flow meters            |                                     |                            |

The extraction reaction of (-)-DBTA with levocetirizine is according to Eq. (1):



where  $k_1$  and  $k_2$  are the apparent rate constants of feed membrane interfacial transport and membrane strip interfacial transport, respectively, of levocetirizine enantiomers. Subscripts f and m are defined as feed phase and membrane phase, respectively.

The complex of levocetirizine-(-)-DBTA diffuses across the membrane phase to the opposite side due to the concentration gradient, and reacted with the stripping agent,  $\text{Cl}^-$ ; then levocetirizine is released to the stripping solution. The stripping equation is shown in Eq. (2):



where  $k_3$  and  $k_4$  are the apparent rate constants of feed membrane interfacial and membrane strip interfacial transport of cetirizine enantiomers, respectively. Subscripts m and s are defined as membrane phase and stripping phase, respectively.

The levocetirizine is transferred to the stripping phase, whereas the extractant returns to the membrane phase and diffuses to the feed-membrane interface due to the concentration gradient in order to react once again with levocetirizine in the feed solution.

The percentage of extraction is identified as follows:

$$\% \text{Extraction} = \frac{C_{f,in} - C_{f,out}}{C_{f,in}} \times 100 \quad (3)$$

The percentage of stripping is calculated by:

$$\% \text{Stripping} = \frac{C_{s,out}}{C_{f,in}} \times 100 \quad (4)$$

where  $C_{f,in}$ ,  $C_{f,out}$  are the inlet and outlet feed concentrations of levocetirizine (mmol/L) and  $C_{s,out}$  is the outlet stripping concentration of levocetirizine (mmol/L).

The selectivity is defined as enantioselectivity. The enantioselectivity of the membrane process is given in terms of enantiomeric excess. The enantiomeric excess is defined by the ratio of the difference between the concentrations of both enantiomers in the feed or stripping phase to the total amount of both enantiomers present at any time, and is calculated according to Eq. (15):

$$\% \text{Enantiomeric excess} = \frac{C_{(S)} - C_{(R)}}{C_{(S)} + C_{(R)}} \times 100 \quad (5)$$

### 1. Extraction Equilibrium Constant and Distribution Ratio

The extraction equilibrium constant ( $K_{ex}$ ) of levocetirizine extracted by (-)-DBTA in Eq. (1) is derived from the experimental data and calculated from Eq. (6). From the extraction reaction described in Eq. (1), the extraction equilibrium constant ( $K_{ex}$ ) can be expressed as:

$$K_{ex} = \frac{[[\text{levocetirizine}]_2(-)\text{-DBTA}]_m}{[\text{levocetirizine}]_f^2 [(-)\text{-DBTA}]_m} \quad (6)$$

The distribution ratio (D) for levocetirizine is given by

$$D = \frac{[[\text{levocetirizine}]_2(-)\text{-DBTA}]_m}{[\text{levocetirizine}]_f} \quad (7)$$

According to Eq. (6), the distribution ratio can then be derived as a function of the extraction equilibrium constant as follows:

$$D = K_{ex} [\text{levocetirizine}]_f [(-)\text{-DBTA}]_m \quad (8)$$

where the value of  $K_{ex}$  for levocetirizine extracted with (-)-DBTA was found to be  $1.0433 \text{ L}^2/\text{mmol}^2$ . The results of the experiment are shown in section 4.5.

### 2. Permeability Coefficient

The transportation of levocetirizine can be expressed in terms of overall mass transfer coefficient (P) as proposed by Danesi [31] in Eq. (9):

$$-V_f \ln\left(\frac{C_f}{C_{f,0}}\right) = AP \frac{\beta}{\beta+1} t \quad (9)$$

where P is the overall mass transfer coefficient (cm/s),  $V_f$  is the volume of the feed ( $\text{cm}^3$ ),  $C_{f,0}$  is the levocetirizine concentration (mol/L) at the initial time ( $t=0$ ),  $C_f$  is the levocetirizine concentration at time t (mol/L), A is the effective area of the hollow fiber module ( $\text{cm}^2$ ) and t is the time (in minutes).

$$\beta = \frac{Q_f}{PL \varepsilon \pi N r_i} \quad (10)$$

$AP(\beta/(\beta+1))$  is the slope of the plot between  $-V_f \ln(C_f/C_{f,0})$  versus t in Eq. (9), and P can be obtained by Eq. (7), where  $Q_f$  is the volumetric flow rate of feed solution ( $\text{cm}^3/\text{s}$ ), L is the length of the hollow fiber (cm),  $\varepsilon$  is the porosity of the hollow fiber (%), N is number of hollow fibers in the module, and  $r_i$  is the internal radius of the hollow fiber module (cm).

To determine mass transfer parameters for levocetirizine enantio-separation by HFSLM, the equation of mass transfer model and overall mass transfer coefficient (P) are employed as in Eq. (9). The overall mass transfer coefficient is composed of three mass transfer resistances, which are the reciprocals of the mass transfer coefficients, as follows:

$$\frac{1}{P} = \frac{1}{k_f} + \frac{r_i}{r_m} \frac{1}{P_m} + \frac{r_i}{r_o} \frac{1}{k_s} \quad (11)$$

where  $r_m$  is the log-mean radius of the hollow fiber,  $r_o$  is the external radius of the hollow fiber module (cm),  $k_f$  is the mass transfer coefficient at feed phase in the tube side,  $k_s$  is the mass transfer coefficient at stripping phase, and  $P_m$  is the membrane permeability coefficient.

The relationship between  $P_m$  and the distribution ratio (D) is as follows [32]:

$$P_m = Dk_m \quad (12)$$

Combining Eq. (8) and Eq. (12), thus

$$P_m = K_{ex} k_m [\text{levocetirizine}]_f [(-)\text{-DBTA}]_m \quad (13)$$

where  $k_m$  is the mass transfer coefficient of organic membrane phase, and the permeability coefficient ( $P_m$ ) from Eq. (13) is substituted into Eq. (11). Assuming that the stripping reaction is instantaneous and the contribution of the stripping phase is neglected [33], therefore, Eq. (11) becomes:

$$\frac{1}{P} = \frac{1}{k_f} + \frac{r_i}{r_m} \frac{1}{K_{ex} k_m [\text{levocetirizine}]_f [(-)\text{-DBTA}]_m} \quad (14)$$

## EXPERIMENT

### 1. Chemicals and Reagents

Pharmaceutical-grade levocetirizine, dextrocetirizine and racemic cetirizine were provided by the Government Pharmaceutical Organization (GPO) of Thailand. *O,O'*-dibenzoyl-(2*R*,3*R*)-tartaric acid ((-)-DBTA) was obtained from Acros Organics (Geel, Belgium). The solvents, i.e., dipotassium hydrogen phosphate, orthophosphoric acid, acetonitrile, *N,N*-dimethylformamide, 1-propanol, 1-decanol and hydrochloric acid, were all of analytical reagent grade and were obtained from Merck, Germany. All reagents used in this experiment were of GR grade and also were purchased from Merck, Germany. Aqueous solutions were prepared using Milli-Q® deionized water (Millipore®, USA). Doubly deionized water was used throughout the experiments.

### 2. Apparatus

The hollow fiber supported liquid membrane (HFSLM) system (Liqui-Cel® Extra-Flow 2.5×8 in membrane contactor) was manufactured by Celgard (formerly Hoechst Celanese), Charlotte NC, USA. The module uses Celgard® microporous polypropylene fibers that are woven into fabric and wrapped around a central tube feeder that supplies the shell-side fluid. The woven fabrics provide more uniform fiber spacing, which in turn leads to higher mass transfer coefficients than those obtained with individual fibers [34]. The properties of the hollow fiber module are specified in Table 1. The fibers were put into a solvent-resistant polyethylene tube sheet with polypropylene shell casing.

### 3. Procedures

The single-module operation is shown in Fig. 2. The selected organic carrier (-)-DBTA was dissolved in 1-decanol (500 mL) and then pumped simultaneously into the tube and shell sides of the hollow fiber module for 40 min to ensure that the extractant was entirely embedded in the micro-pores of the hollow fibers. Subsequently, 5 L (each) of feed solution and stripping solution was fed counter-currently into the tube and shell sides of the module.

**Table 1. The characteristics of the hollow-fiber module**

Properties	Descriptions
Material	Polypropylene
Dimension of module (diameter x length)	6.3×20.3 cm
Inside diameter of hollow fiber	240 μm
Outside diameter of hollow fiber	300 μm
Effective length of hollow fiber	15 cm
Number of hollow fibers	35,000
Average pore size	0.03 μm
Size of pore	0.05 μm
Porosity	30%
Effective surface area	1.4×10 <sup>4</sup> cm <sup>2</sup>
Area per unit volume	29.3 cm <sup>2</sup> /cm <sup>3</sup>
Module diameter	6.3 cm
Module length	20.3 cm
Contact area	1.4 m <sup>2</sup>
Tortuosity factor	2.6
Maximum pressure difference	4.2 kg/cm <sup>2</sup>
Operating temperature	273.15-333.15 K

The concentration of feed solution was deliberately varied to find the optimum value for levocetirizine extraction. The concentration of the chiral selector (-)-DBTA in the liquid membrane, volumetric flow rates of feed and stripping solutions, the number of separation cycles, and stability of the HFSLM were each investigated in turn. The operating time for each run was 50 min. The concentrations of levocetirizine in samples from the feed and stripping solutions were determined by high-performance liquid chromatography (HPLC) to estimate the percentages of extraction and stripping. Levocetirizine and dextrocetirizine were determined using an HPLC method, essentially as described by Benedetti et al. [35] with some modification. To achieve higher enantioseparation and to study membrane stability, the number of separation cycles was increased.

### 4. Analytical Instruments and Chromatographic Conditions

The levocetirizine and dextrocetirizine concentrations were analyzed by HPLC, essentially as described by Benedetti et al. [35] with some modification. The chromatographic system consisted of an Agilent 1100 series compact LC system (Agilent Technologies, Palo Alto, CA, USA), equipped with a built-in solvent degasser, quaternary pump, column compartment, photodiode array detector with variable injector, and autosampler. The data was gathered using ChemStation Version B.04.01 software (Agilent). Agilent Ultron ES-OVM ovomucoid chiral column (5 μm, 4.6×150 mm) was used for chromatographic procedure [33]. The column was thermostated at 308.15 K. The compositions of the mobile phase were as follows: solvent A consisted of dipotassium hydrogen phosphate (0.10 mol/L) adjusted to pH 6.5 using orthophosphoric acid/acetonitrile (95/5 : v/v), and solvent B consisted of dipotassium hydrogen phosphate (0.10 mol/L) adjusted to pH 6.5 using orthophosphoric acid/acetonitrile (75/25 : v/v). Isocratic elution (30% B) was performed. The flow rate of the mobile phase was 1.0 mL/min and injection volume was 20 μL. The relative retention times of dextrocetirizine and levocetirizine were about 1.00 and 1.28, respectively, with the UV detector set at 230 nm. The analysis time was set at 20 min per sample to eliminate potential interference from late eluting peaks. The pH of the aqueous phase was measured with a SevenMulti™ modular pH meter with expansion unit (Mettler-Toledo, Greifensee, Switzerland).

## RESULTS AND DISCUSSION

### 1. Effect of the (Initial) pH of the Feed Phase

The effect of pH of feed phase on the distribution behavior of enantiomers was examined. The HFSLM was operated in recirculation mode with 4 mmol/L of (-)-DBTA in 1-octanol solvent and 4 mmol/L racemic levocetirizine. The pH is an important factor for the ionized form of levocetirizine enantiomers. Due to its zwitterionic nature, cetirizine can be considered as a cation at pH 3.0 and as an anion at pH 9.0. For these experiments two buffer solutions were used: 50 mmol/L tri-ethanolamine-phosphate buffer, pH 3.0, and 20 mmol/L sodium tetraborate buffer, pH 9.0. Although no chiral separation could be observed under all tested conditions, the migration of cetirizine significantly increased below pH 3.0. The increasing of the initial pH of the feed phase led to a decrease in resolution and even a complete loss of resolution at pH 4.0. The separation of the enantiomers is based on inclusion complexation and is extra stabilized with electrostatic interaction between the positively charged

nitrogens of the levocetirizine and the negatively charged carboxylic group of the chiral selector. At pH 3.0 and higher, the carboxylic function on cetirizine will be negatively charged. Therefore, repulsion between the levocetirizine and the chiral selector can occur, leading to a decrease in resolution. To eliminate all negative charges and therefore possible repulsive forces, pH 2.5 was tested. The beginning of chiral separation could be observed by using a chiral selector.

The pH 2.5 was an appropriate choice in view of the greater enantioselectivity of the separation. This result was in agreement with an earlier report by Mikuš et al. [20], in which carboxyethyl- $\beta$ -cyclodextrin or sulfated- $\beta$ -cyclodextrin was used as a chiral selector at low pH. Further investigations were therefore performed using a 50 mmol/L tri-ethanolamine-phosphate buffer pH 2.5.

## 2. Effect of Chiral Selector Concentration in the Membrane Phase

Fig. 3 shows the effect of chiral selector concentration in the membrane phase on percentages of extraction, stripping, and enantiomeric excess. The concentrations of (-)-DBTA were studied at 2, 4, 6, 8 and 10 mmol/L. The levocetirizine extraction increased with an increase in extractant concentration. At 4 mmol/L, the highest per-

centage of levocetirizine extraction reached 75.00%. Therefore, it was selected as the optimal concentration to be used in further experiments. However, levocetirizine extraction apparently decreased when (-)-DBTA concentrations were higher than 4 mmol/L. The results were in agreement with a previous report by Sunsandee et al. [36].

## 3. Effect of the Flow Rate of Feed Solution

The flow rate of the feed solution plays an important role in the percentages of extraction and stripping of levocetirizine. Fig. 4 shows the relationships between the percentages of extraction and stripping of levocetirizine and the enantiomeric excess at different flow rates of feed and stripping solutions. The flow rates were between 50 to 200 mL/min. The extractant was 4 mmol/L (-)-DBTA. The results indicated that by using a flow rate of feed solution of 100 mL/min, the extraction of levocetirizine reached the highest percentage of 75.00%. Higher flow rates result in less residence time of the solutions, or less contact time of the relevant molecule in the reaction in the HFSLM process. For instance, at too high a flow rate at 200 mL/min, the membrane system may deteriorate. This can be seen from both poor liquid membrane stability and lower percentage of extraction [35,36].

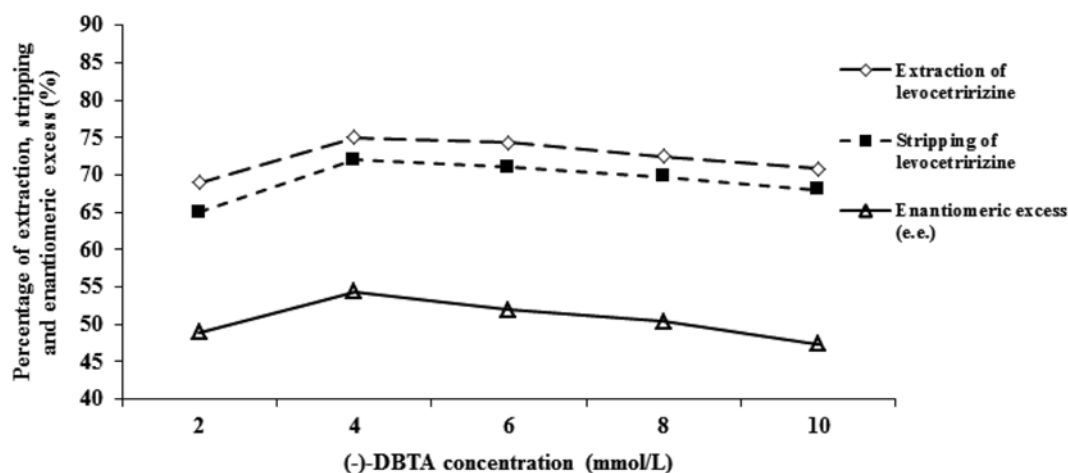


Fig. 3. The effects of (-)-DBTA concentration in the feed phase on percentages of extraction and recovery of levocetirizine and the enantiomeric excess (% e.e.).

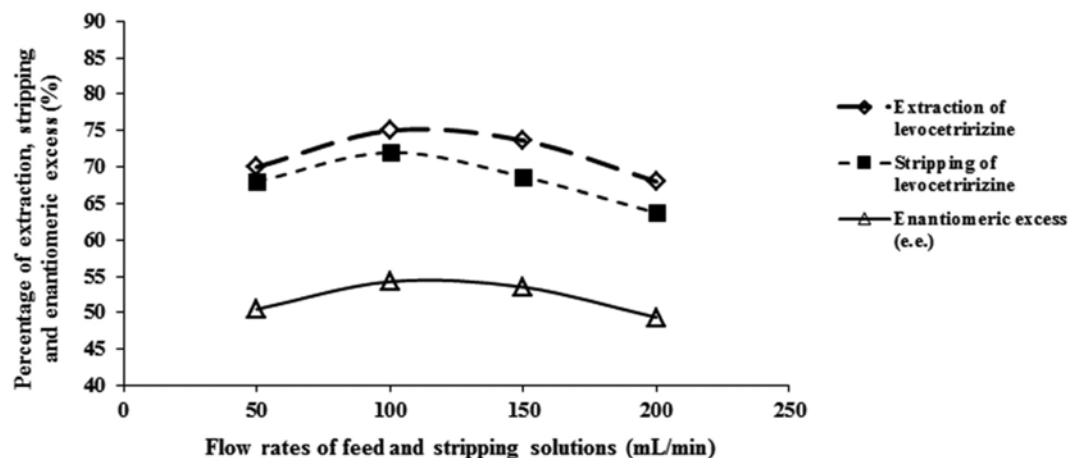


Fig. 4. The effects of the flow rate of feed and stripping solution on percentages of extraction and recovery of levocetirizine and the enantiomeric excess (% e.e.).

#### 4. Effect of the Flow Rate of Stripping Solution

The results in Fig. 4 indicate that the highest stripping of levocetirizine was 72.00% at a flow rate of stripping solution of 100 mL/min. However, both the percentages of extraction and stripping decreased with an increasing of the flow rates of feed and stripping solutions due to residence time of solutions in the hollow fiber module [33].

#### 5. Extraction Equilibrium Constant and Distribution Ratio

The extraction equilibrium constant ( $K_{ex}$ ) described in Eq. (6) was calculated from the slope of the plot between  $[\text{levocetirizine}]_f^2$   $[(\text{-})\text{-DBTA}]$  and  $[[\text{levocetirizine}]_2\text{-}(\text{-})\text{-DBTA}]_m$ , and was found to be 1.0433 L/mm<sup>2</sup>. The distribution ratio (D) at a levocetirizine concentration of 4 mmol/L was calculated by Eq. (9), as shown in

**Table 2. The distribution ratio (D) at the (-)-DBTA concentrations in the range 2, 4, 6, 8 and 10 mmol/L**

[(-)-DBTA] (mmol/L)	2	4	6	8	10
The distribution ratio	1.02	2.13	3.07	4.05	5.06

Table 2. It should be noted that the distribution ratio increased with the extractant concentration [37].

#### 6. Permeability and Mass Transfer Coefficients

The overall mass transfer coefficients of levocetirizine at different concentrations of (-)-DBTA, from 2 to 8 mmol/L, were calculated by the slope obtained in Fig. 5, as shown in Table 3. The results show that the overall mass transfer coefficient increased with the extractant concentration. Eq. (14) was obtained by substituting the membrane permeability coefficient ( $P_m$ ) in Eqs. (10) and (11) into

**Table 3. Permeability coefficients (P) at (-)-DBTA concentrations of 2, 4, 6 and 8 mmol/L**

Concentration of (-)-DBTA (mmol/L)	Permeability coefficient (cm/s)
2	1.15
4	1.47
6	1.71
8	1.95

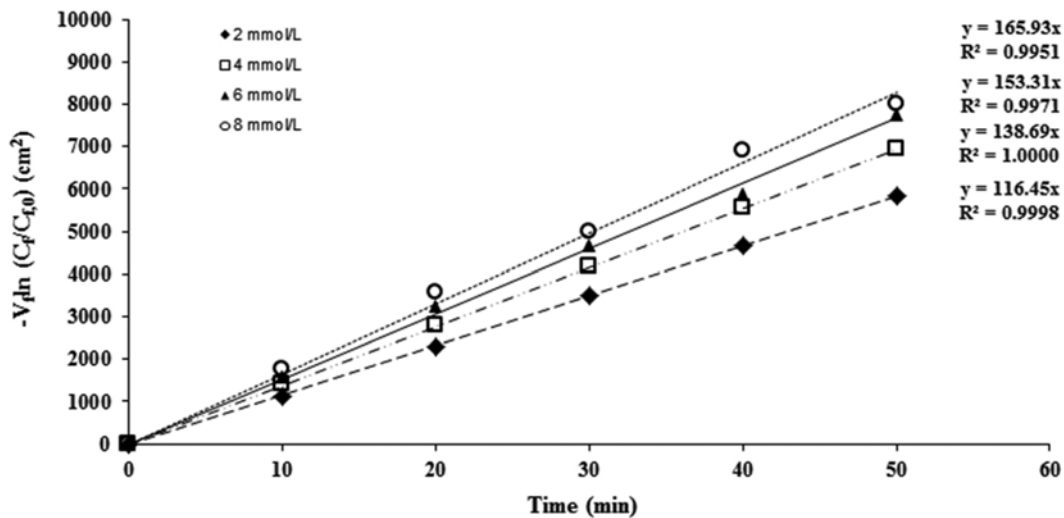


**Fig. 5. The plot of  $-V_f \ln(C_f/C_{f,0})$  of levocetirizine in the feed solution against time with different (-)-DBTA concentrations.**

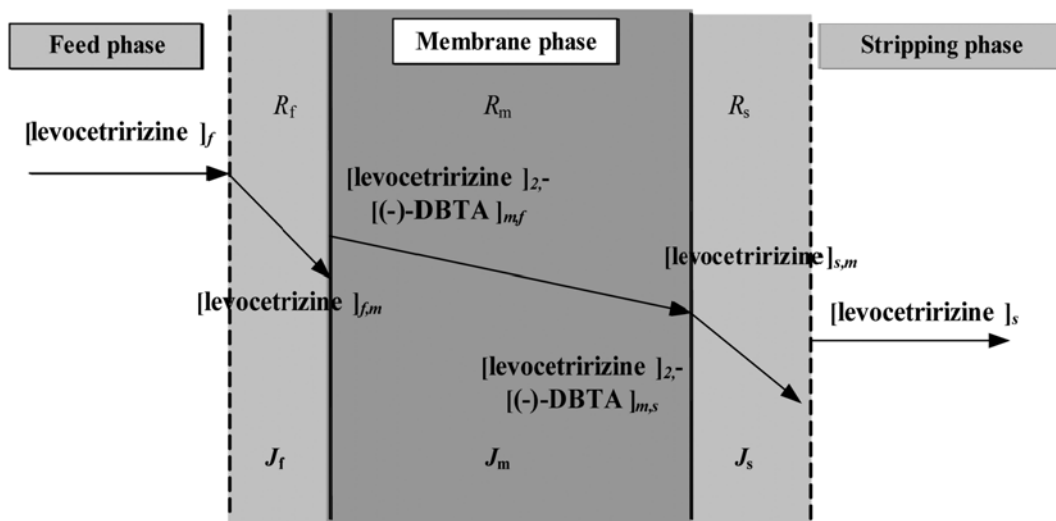


**Fig. 6. Mass transfer of levocetirizine with (-)-DBTA and concentration profile in HFSLM.**

Eq. (9), assuming that the stripping reaction of levocetirizine was instantaneous and that there was no contribution of the stripping phase. Eq. (14) was used to calculate the aqueous mass transfer coefficient ( $k_f$ ) and the membrane mass transfer coefficient ( $k_m$ ). By plotting  $1/p$  as a function of  $1/(K_{ex} k_m [\text{levocetirizine}]_f [(-)\text{-DBTA}]_m)$  in different carrier concentrations of (-)-DBTA (shown in Fig. 5), a straight line with slope  $r_f/r_m$   $1/K_{ex} k_m$  was obtained with an ordinate of  $1/k_f$ . Thus,  $k_f$  and  $k_m$  were found to be  $2.41 \times 10^2$  and  $1.89 \times 10^2$  cm/s, respectively.

### 7. Enantiomeric Flux Modeling of Levocetirizine Concentration

The levocetirizine concentration profile through HFSLM is shown in Fig. 6.

The diffusive mass transport flux is modeled under the following assumptions:

- 1) The system is considered to be at pseudo-steady state.
- 2) The extraction reaction takes place at the interface between the aqueous solution and the liquid membrane. The influence of the interface curvature on the mass transfer can be neglected.
- 3) No solute transport occurs through the non-porous parts of the membrane.
- 4) Mass transfer is described by simple film-type mass transport coefficients.

The objective of the mathematical model is to calculate the overall levocetirizine flux ( $J$ ) from the feed phase to the organic phase, as defined as follows:

$$J_f R_f = [\text{levocetirizine}]_{f,0} - [\text{levocetirizine}]_{f,m} \quad (15)$$

$$J_m R_m = [\text{levocetirizine}]_{m,f} - [\text{levocetirizine}]_{m,s} \quad (16)$$

$$J_s R_s = [\text{levocetirizine}]_{s,m} - [\text{levocetirizine}]_{s,0} \quad (17)$$

where  $R_m = 1/k_m$  and  $R_f = 1/k_f$  are the membrane and aqueous mass transfer resistance, respectively, and  $[\text{levocetirizine}]_{f,0}$ ,  $[\text{levocetirizine}]_{f,m}$  are the concentrations of the levocetirizine complexes in the feed solution and at the interface between aqueous feed solution and membrane phase at subsequent time  $t$ .

By considering the extraction reaction in Eq. (1),  $[\text{levocetirizine}]_{f,m}$  is the concentration of the levocetirizine in the interface between aqueous feed phase and membrane phase and  $[\text{levocetirizine}]_{m,f}$  is the concentration of the levocetirizine complex in the membrane phase, as follows:

$$[\text{levocetirizine}]_{m,f} = [(\text{levocetirizine})_2(-)\text{-DBTA}]_m \quad (18)$$

From Eq. (6),  $[\text{levocetirizine}]_{m,f}$  is defined in terms of the equilibrium constant  $K_{ex}$ ,

$$[\text{levocetirizine}]_{m,f} = K_{ex} [\text{levocetirizine}]_{f,m}^2 [(-)\text{-DBTA}] \quad (19)$$

The flux equation of the diffusion of the  $(\text{levocetirizine})_2(-)\text{-DBTA}$  complex through the membrane phase can be written as Eq. (15). The concentration of the strip solution was much lower than the feed phase [38]. Thus, can be neglected. Therefore:

$$J_m R_m = [\text{levocetirizine}]_{m,f} \quad (20)$$

$[\text{levocetirizine}]_{m,f}$  from Eq. (19) was substituted into Eq. (20) to obtain the following expression:

$$[\text{levocetirizine}]_{f,m}^2 = \frac{J_m R_m}{K_{ex} [(-)\text{-DBTA}]} \quad (21)$$

Under the pseudo-steady-state condition assumption that  $J_m = J_f = J$ , the equation flux from Eq. (15) can be expressed as follows:

$$[\text{levocetirizine}]_{f,m}^2 = ([\text{levocetirizine}]_{f,0} - JR_f)^2 \quad (22)$$

By substituting  $[\text{levocetirizine}]_{f,m}^2$  from Eq. (21) into Eq. (22), the result can be rearranged into a quadratic equation:

$$J^2 R_f^2 - J \left( 2R_f [\text{levocetirizine}]_f + \frac{R_m}{K_{ex} [(-)\text{-DBTA}]} \right) + [\text{levocetirizine}]_f^2 = 0 \quad (23)$$

Because  $(2R_f [\text{levocetirizine}]_f + \frac{R_m}{K_{ex} [(-)\text{-DBTA}]} \gg$

$$\sqrt{\left[ - \left( 2R_f [\text{levocetirizine}]_f + \frac{R_m}{K_{ex} [(-)\text{-DBTA}]} \right)^2 \right] - 4R_f^2 [\text{levocetirizine}]_f^2}$$

the term

$$\sqrt{\left[ - \left( 2R_f [\text{levocetirizine}]_f + \frac{R_m}{K_{ex} [(-)\text{-DBTA}]} \right)^2 \right] - 4R_f^2 [\text{levocetirizine}]_f^2}$$

can be neglected.

Eventually, the enantiomeric flux is:

$$J = \frac{[\text{levocetirizine}]_f}{R_f} + \frac{R_m}{2K_{ex} R_f^2 [(-)\text{-DBTA}]} \quad (24)$$

From the definition of mass flux given in Reference [39], the equation flux of levocetirizine can be presented as:

$$J = - \frac{d[\text{levocetirizine}]_f V}{dt} \frac{V}{A} \quad (25)$$

where  $V$  is volume of the feed solution ( $\text{cm}^3$ ) and  $A$  is membrane area ( $\text{cm}^2$ ). By combining Eqs. (24) and (25), the following equation is obtained:

$$- \frac{d[\text{levocetirizine}]_f V}{dt} \frac{V}{A} = \frac{R_m}{2K_{ex} R_f^2 [(-)\text{-DBTA}]} + \frac{[\text{levocetirizine}]_f}{R_f} \quad (26)$$

Finally, by integrating with initial conditions  $t=0$  and  $[\text{levocetirizine}]_f = [\text{levocetirizine}]_{f,0}$ , the equation for levocetirizine concentration in the feed tank at different times can be expressed as:

$$[\text{levocetirizine}]_f = - \frac{R_m}{2K_{ex} R_f^2 [(-)\text{-DBTA}]} + \left( \frac{R_m}{2K_{ex} R_f [(-)\text{-DBTA}]} \right) \exp\left(- \frac{A}{VR_f} t\right) \quad (27)$$

The mass transfer reaction of levocetirizine through a hollow fiber supported liquid membrane was assessed by enantiomeric flux modeling, as represented in Fig. 7. Eq. (27) was used to predict the concentration of levocetirizine at different times for different extractant concentrations of 2, 4, 6, 8 and 10 mmol/L. The computational results shown by the solid line were in good agreement with the experimental data (dashed line). The diffusion process started by Fick's law of diffusion and mass transfer flux was established in this mathematical model. Therefore, it can be concluded that the enantiomeric flux model is satisfactory for the separation of levocetirizine through

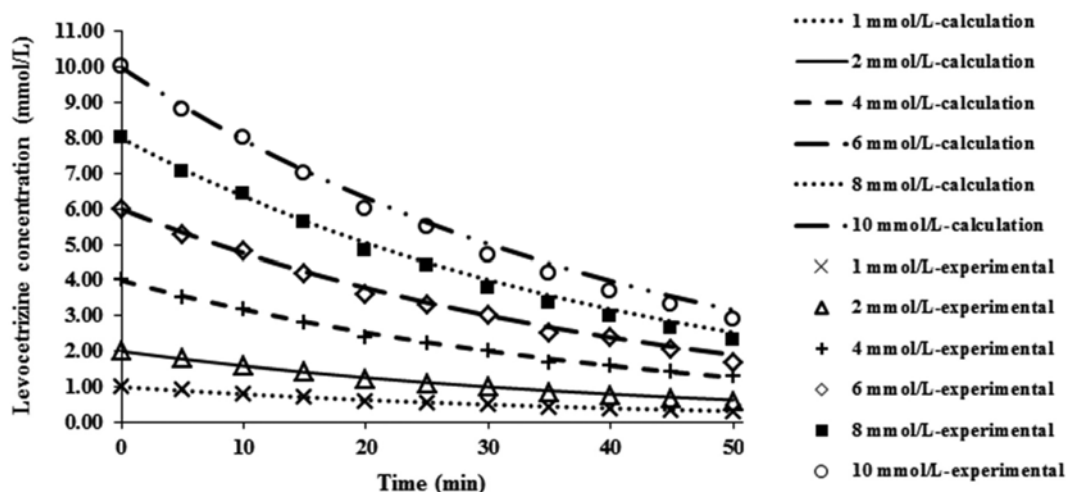


Fig. 7. Different concentrations of levocetirizine in the feed phase plotted as a function of time.

a hollow fiber supported liquid membrane. It is a simple mathematical model which can be easily used to predict the concentration of enantioseparation in the feed tank for the recirculating mode of an HFSLM system.

### CONCLUSIONS

Enantioseparation of racemic cetirizine containing (-)-DBTA as a chiral carrier via hollow fiber supported liquid membrane was carried out successfully by HFSLM system. The levocetirizine percentages of cumulative extraction and cumulative stripping were 75.00% and 72.00%, respectively, from an initial concentration of feed solution of 4 mmol/L, chiral carrier ((-)-DBTA) of 4 mmol/L, 100 mL/min of feed and stripping solutions. The mass transfer coefficients of the aqueous phase ( $k_f$ ) and organic phase ( $k_m$ ) are  $2.41 \times 10^2$  and  $1.89 \times 10^2$  cm/s, respectively. The mathematical model can predict the concentration of levocetirizine in the feed tank because the computational values are in good agreement with the experimental results.

### ACKNOWLEDGEMENTS

The authors greatly appreciate financial support from the Department of Chemical Engineering, Faculty of Engineering and Industrial Technology, Silpakorn University, Nakhon Pathom, Thailand. Sincere thanks also to the Government Pharmaceutical Organization (GPO), Thailand, for kindly supplying active pharmaceutical ingredients and all instruments for analysis and measurement.

### NOMENCLATURE

C	: concentration [mmol/L]
$k_f$	: aqueous feed mass transfer coefficient [cm/s]
$k_m$	: membrane mass transfer coefficient [cm/s]
$K_{ex}$	: extraction equilibrium [-]
P	: permeability coefficient [cm/s]
$P_m$	: membrane permeability [cm/s]
A	: effective area of hollow fiber [cm <sup>2</sup> ]
$V_f$	: volume of feed phase [cm <sup>3</sup> ]

$r_m$	: log-mean radius of the hollow fiber [cm]
$r_i$	: internal radius of the hollow fiber [cm]
$r_o$	: external radius of the hollow fiber [cm]
Q	: volumetric flow rate [cm <sup>3</sup> /s]
L	: length of the hollow fiber [cm]
N	: number of hollow fibers in module [-]
$R_m$	: membrane mass transfer resistance [s/cm]
$R_f$	: aqueous feed mass transfer resistance [s/cm]
t	: time [min]
T	: temperature [K]

### Greek Letters

$\tau$	: tortuosity of membrane [-]
$\varepsilon$	: porosity of membrane [-]
$\eta$	: viscosity of the liquid membrane [kg/(s·m)]

### Subscripts

f	: feed phase
s	: stripping phase
m	: membrane phase
i	: inter phase

### REFERENCES

1. J. Bousquet, P. V. Cauwenberge and N. Khaltaev, *J. Allergy Clin. Immunol.*, **108**, 147 (2001).
2. M. M. A. Kozel and R. A. Sabroe, *Drugs*, **64**, 2515 (2004).
3. M. W. Greaves, *Allergy Clin. Immunol.*, **3**, 363 (2003).
4. J. H. Day, A. K. Ellis and E. Rafeiro, *Drugs Today*, **40**, 415 (2004).
5. M. Gillard, C. V. Perren, N. Moguelevsky, R. Massingham, P. Chatelain, *Inflamm. Res.*, **51**, 79 (2002).
6. M. Gillard and P. Chatelain, *Eur. J. Pharmacol.*, **530**, 205 (2006).
7. D. M. Campoli-Richards, M. M. T. Buckley and A. Fitton, *Drugs*, **40**, 762 (1990).
8. J. P. Tillement, B. Testa and F. Bree, *Biochem. Pharmacol.*, **66**, 1123 (2003).
9. M. P. Curran, L. J. Scott and C. M. Perry, *Drugs*, **64**, 523 (2004).
10. A. Pagliara, B. Testa, P. A. Carrupt, P. Jolliet, C. Morin, D. Morin, S. Urien, J. P. Tillement and J. P. Rihoux, *J. Med. Chem.*, **41**, 853

- (1998).
11. J. L. Devalia, D. V. Christine, F. Hanotte and E. Baltes, *Allergy*, **56**, 50 (2001).
  12. P. I. Hair, L. J. Scott, *Drugs*, **66** (2006).
  13. F. E. Simons, *N. Engl. J. Med.*, **351**, 2203 (2004).
  14. J. A. Grant, J. M. Riethuisen, M. Béatrice and D. V. Christine, *Ann. Allergy Asthma Immunol.*, **88**, 190 (2002).
  15. M. R. Morita, D. Berton, R. Boldin, F. A. Barros, E. C. Meurer, A. R. Amarante, D. R. Campos, S. A. Calafatti, R. Pereira, E. Jr. Abib and J. Jr. Pedrazolli, *J. Chromatogr. B Anal. Technol. Biomed. Life Sci.*, **862**, 132 (2008).
  16. M. S. Arayne, N. Sultana and M. Nawaz, *J. Anal. Chem.*, **63**, 881 (2008).
  17. L. Zelikovitch and H. Shaked, US Patent Application US20110230496A1 (2011).
  18. N. J. Turner, *Nat. Chem. Biol.*, **5**, 567 (2009).
  19. E. A. Taha, N. N. Salama and S. Wang, *Drug. Test. Anal.*, **1**, 118 (2009).
  20. P. Mikuš, K. Maráková, I. Valásková and E. Havránek, *Pharmazie*, **64**, 423 (2009).
  21. J. Tihi, R. Zupet, A. Pecavar, I. Kolenc and D. Pavlin, US Patent Application US20100105908 (2010).
  22. M. T. Reetz, L. W. Wang and M. Bocola, *Angew. Chem. Int. Ed.*, **45**, 1236 (2006).
  23. U. Pancharoen, S. Somboonpanya, S. Chaturabul and A. W. Lothongkum, *J. Alloy Compd.*, **489**, 72 (2010).
  24. U. Pancharoen, P. Ramakul and W. Patthaveekongka, *J. Ind. Eng. Chem.*, **11**(6), 926 (2005).
  25. A. W. Lothongkum, P. Ramakul, W. Sasomsub, S. Laoharochanapan and U. Pancharoen, *J. Taiwan Inst. Chem. Eng.*, **40**, 518 (2009).
  26. J. D. Rogers and R. Long, *J. Membr. Sci.*, **134**, 1 (1997).
  27. L. Giorno and E. Drioli, *Membr. Technol.*, **106**, 6 (1999).
  28. F. Valenzuela, C. Basualto and C. Tapia, *J. Membr. Sci.*, **155**, 163 (1999).
  29. R. S. Juang, R. H. Huang and R. T. Wu, *J. Membr. Sci.*, **136**, 1 (1997).
  30. H. Murakami, *Top. Curr. Chem.*, **269**, 273 (2007).
  31. P. R. Danesi, *J. Membr. Sci.*, **20**, 231 (1984).
  32. N. S. Rathore, J. V. Sonawane, Anilkumar, A. K. Venugopalan, R. K. Singh, D. D. Bajpal and J. P. Shukla, *J. Membr. Sci.*, **189**, 119 (2001).
  33. P. Wannachod, S. Chaturabul, U. Pancharoen, A. W. Lothongkum and W. Patthaveekongka, *J. Alloy. Compd.*, **509**, 354 (2011).
  34. U. Pancharoen, T. Wongsawa and A. W. Lothongkum, *Sep. Sci. Technol.*, **46**, 2183 (2011).
  35. M. S. Benedetti, M. Plisnier, J. Kaise, L. Maier, E. Baltes, C. Arendt and N. McCracken, *Eur. J. Clin. Pharmacol.*, **57**, 571 (2001).
  36. N. Sunsandee, N. Leepipatpiboon, P. Ramakul and U. Pancharoen, *Chem. Eng. J.*, **180**, 299 (2012).
  37. P. Ramakul, E. Songkun, W. Pattaweekongka, M. Hronec and U. Pancharoen, *Korean J. Chem. Eng.*, **23**(1), 117 (2006).
  38. F. Z. El Aamrania, A. Kumara, L. Beyerb, A. Floridoa and A. M. Sastrea, *J. Membr. Sci.*, **152**, 263 (1999).
  39. S. H. Lin and R. S. Juang, *J. Membr. Sci.*, **188**, 251 (2001).